

Shell Model in the Lead Region*

Chin W. Ma† and William W. True

Physics Department, University of California, Davis, California 95616

(Received 4 October 1972)

The structure of the low-lying states in ^{206}Pb , ^{210}Pb , ^{210}Po , ^{208}Bi , ^{210}Bi , ^{208}Tl , ^{206}Tl , and ^{206}Hg has been calculated using a conventional shell-model approach with a central Gaussian-shaped interaction plus P_2 and P_3 multipole interactions where the P_2 and P_3 strengths were varied for each nucleus. The results are compared with the experimental data and other calculations. The agreements between the experimental energies and spectroscopic factors and the calculations are in general good. The agreements between the experimental and calculated $E2$ and $M1$ rates in ^{206}Pb and ^{210}Po are also fairly good.

I. INTRODUCTION

The lead region, especially those nuclei close to the doubly magic ^{208}Pb nucleus, continues to be one of the better regions in the Periodic Table in which to use the conventional shell model. It is also a region where one can expect to be able to test new models as well as testing modifications and/or extensions of the shell model. Consequently many nuclear-structure calculations have been done in this region in the past few years. Most, but not all, of the calculations done in the lead regions in recent years can be found in Refs. 1–23 and in references contained in these papers. The papers cited above deal with calculations on or related to the structure of the nuclei ^{206}Pb , ^{210}Pb , ^{210}Po , ^{208}Bi , ^{210}Bi , ^{208}Tl , ^{206}Tl , and ^{206}Hg and these nuclei will be discussed in this paper.

The experimental effort in the lead region has also intensified in the past few years. This increased research in the lead region has become feasible by better accelerators with increased intensity and improved resolution along with solid-state detectors which also have improved resolution so that the closely lying excited levels in the lead region can be resolved and studied. Most of the experimental investigations on the above mentioned nuclei can be found in Refs. 24–66 and in references contained in these papers.

In this paper, calculations will be described which use a conventional shell model for the eight nuclei ^{206}Pb , ^{210}Pb , ^{210}Po , ^{208}Bi , ^{210}Bi , ^{208}Tl , ^{206}Tl , and ^{206}Hg . Calculations on the structure of ^{208}Pb have been reported by True, Ma, and Pinkston,¹ hereafter referred to as TMP, and will not be discussed in detail in this paper.

In Sec. II, the residual force used will be discussed in some detail, while remarks on the single-particle orbits will be made. In Sec. III, the results of the calculations for each of the eight nuclei will be presented, compared with the known

experimental data on these nuclei, and also compared with other theoretical calculations.

In this paper, it is to be stressed that conventional shell-model calculations were done. These calculations do not include any additional refinements such as the random-phase approximation²¹ or any explicit renormalization of the matrix elements due to core excitation and/or model-space truncation^{22, 67} even though they may have been implicitly included in the effective residual interaction used.

II. RESIDUAL FORCE

The residual force is expected to depend on the model space^{67, 68} used since a truncation of the basis states is always necessary in any numerical calculation. As was done in TMP, the proton single-particle (hole) orbitals will be restricted to those orbitals in the major shell just above (below) the magic number of $Z=82$. Likewise, the neutron single-particle (hole) orbitals will be restricted to those orbitals in the major shell just above (below) the magic number of $N=126$. In particular, the $A=210$ nuclei were restricted to two-particle configurations, the $A=208$ nuclei were restricted to one-hole-one-particle configurations, and the $A=206$ nuclei were restricted to two-hole configurations. These single-particle orbitals and their relative spacings, spins, parities, etc.,⁵⁵ are shown in Fig. 1.

Furthermore, the radial part of the single-particle orbitals will be assumed to have a harmonic-oscillator shape with $\nu=0.1842\text{ fm}^{-2}$ since it is believed that this choice of the radial wave functions gives a fairly good estimate of the radial part of the matrix elements of the residual interaction. See TMP, Sec. IIIA for further details.

In TMP, Sec. IIIB, a residual interaction consisting of a singlet-even central interaction, V_{SE} , a triplet-even central interaction, V_{TE} , and a weak-

coupling interaction, V_{WC} , was found which gave a fairly complete description of the low-lying negative-parity states in ^{208}Pb .

The weak-coupling interaction, V_{WC} , can be considered from several somewhat different points of view. In True and Ford² and in True,³ this weak-coupling interaction was assumed to arise from the weak coupling of the lower-lying orbitals to a rather high-lying $L=2$ collective phonon-type state. V_{WC} is like a P_2 multipole interaction which does not have an explicit radial dependence since the radial part of the matrix elements is replaced by a constant, k^2/C , which is some suitably averaged radial matrix element depending in general on the detailed properties of the collective state.

Kuo and Brown⁹ have indicated that when model-space truncation effects are considered, then the residual force should be modified from the free nucleon-nucleon interaction by the addition of a P_2 multipole interaction and even possibly by the addition of a P_4 multipole interaction. A P_L multipole interaction means an interaction of the form

$$V_L = \alpha_L r_1^L r_2^L P_L(\cos\theta_{12}). \quad (1)$$

The low-lying levels of ^{206}Pb were calculated by the authors with the interaction $V_{SE} + V_{TE} + V_{WC}$ from TMP and with the interaction $V_{SE} + V_{TE} + V_{L=2}$ where

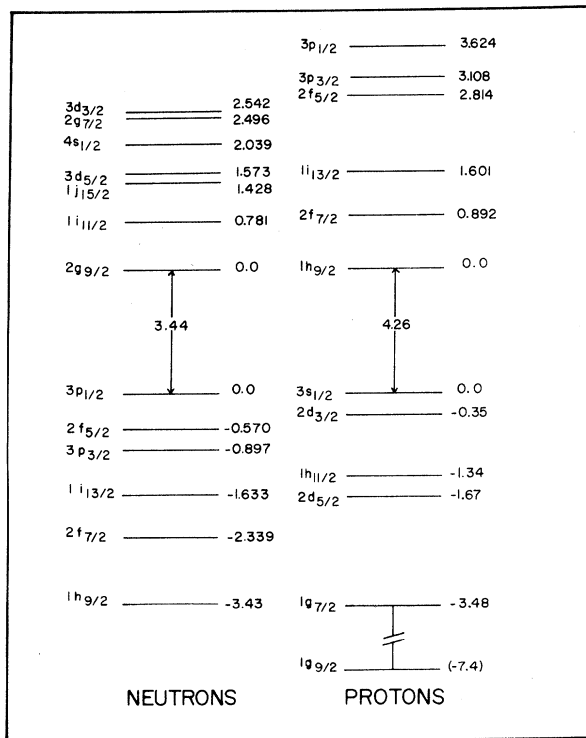


FIG. 1. The experimental single-particle spacings in MeV in the lead region from Ref. 55.

the V_{SE} and V_{TE} potentials were the same in both cases and α_2 was varied to obtain the best fit to the energy levels. Both calculations gave essentially the same description of the low-lying states of ^{206}Pb . One thus can conclude that the results are somewhat insensitive to whether a weak-coupling interaction, V_{WC} , or a P_2 multipole interaction is used.

It was also shown in TMP that the very collective 3^- level at 2.6 MeV in ^{208}Pb can be very well described in terms of neutron and proton particle-hole states constructed from the single-particle orbitals shown in Fig. 1. This level has often been referred to as a collective $L=3$ type phonon state. From the "phonon" point of view, orbitals could be vector-coupled weakly to this $L=3$ collective phonon state.² If this were the case, one might expect effects from this coupling to show up in the properties of low-lying levels in the lead region. Note that one cannot take this point of view if the configurations which give rise to this collective 3^- level are explicitly included in the model space considered. For example, in the calculation of ^{208}Pb described in TMP, any coupling to this 3^- state would be explicitly included in the calculation providing this state can be described by one hole-one particle configurations of $1\hbar\omega$ excitation.

The calculations in this paper for eight nuclei in the lead region do not explicitly include in the model space the particle-hole states which are believed to give rise to this collective 3^- level. It seems reasonable in these cases that any coupling to this collective 3^- level could be described for the most part by the addition of a $L=3$ weak-coupling interaction. Or one could argue that these model-space truncation effects could be accounted for by a P_3 multipole interaction. Since either of the above $L=2$ type interactions worked equally well in ^{206}Pb , it also seems quite reasonable that either type of the above $L=3$ interactions would also work equally well in the lead region. Currently the multipole interaction is favored by many physicists since its strength can be estimated by the Kuo-Brown microscope approach, whereas a microscopic description of the collective-type phonon states is on less firm grounds.

In this paper, the choice of the residual force(s) will be based on several aspects. It should be emphasized that providing one is not too concerned about a few levels, one to three levels per nucleus on the average, differing from the experimental values by about 200 keV, a Gaussian-shaped central force of the form

$$V = V_0 e^{-\beta r^2} (P^{SE} + \eta P^{TE}), \quad (2)$$

where P^{SE} and P^{TE} are the singlet-even and triplet-even projection operators, respectively, gives a

fairly good description of the low-lying energy levels of all the nuclei in the lead region which are considered in this paper.

On the other hand, one does not expect the residual force to be the same for all nuclei because different model spaces are being considered for each nucleus. The results of Kuo⁶⁹ and the weak-coupling phonon model¹⁻³ indicate that some of the multipole components of the residual force are more sensitive to model-space truncation than are other components. The calculations described in this paper show that by simply adding P_2 and P_3 multipole forces to the Gaussian-shaped central force above, practically all the low-lying calculated and experimentally observed energy levels can be made to agree with each other to less than 100 keV. In addition, adjustment of these two multipole components also improves the ground-state wave functions of ^{206}Pb and ^{210}Pb as will be discussed later.

Being motivated by the discussion above, we will use in this paper a residual interaction of the form

$$V = (V_0 e^{-\beta r^2} + \mathfrak{U}_{L=2} + \mathfrak{U}_{L=3}) (P^{SE} + \eta P^{TE}), \quad (3)$$

where \mathfrak{U}_L is defined in Eq. (1). The parameters⁵⁶ $V_0 = -22.75$ MeV, $\beta = 0.2922$ fm⁻², and $\eta = 1.8$ are considered to be fixed by the ^{208}Pb calculation described in TMP. The parameters α_2 and α_3 in the $\mathfrak{U}_{L=2}$ and $\mathfrak{U}_{L=3}$ terms of the residual interaction will be the only two adjustable parameters which will be permitted to vary depending on the nucleus being considered.

The values of α_2 and α_3 which gave the best fits to the low-lying levels in the eight nuclei considered in this paper are given in Table I. In most cases, the parameters α_2 and α_3 were adjusted to give the best fits to the observed energy levels. However, in some cases as will be discussed be-

TABLE I. The strengths α_2 and α_3 of the P_2 and P_3 multipole forces which give the best fit in the lead region. p (n) refers to proton (neutron) particles outside the ^{208}Pb core, while \bar{p} (\bar{n}) refers to proton (neutron) holes in the ^{208}Pb core.

Nucleus	α_2	α_3
	(10^{-4} MeV/fm ⁴)	(10^{-4} MeV/fm ⁶)
^{206}Pb (\bar{n}^2)	-5.0	-0.50
^{210}Pb (n^2)	0.0	-0.65
^{210}Po (p^2)	-2.5	-1.20
^{208}Bi ($p\bar{n}$)	0.0	-1.95
^{210}Bi ($p n$)	+5.5	-0.55
^{208}Tl ($\bar{p} n$)	-2.5	-1.50
^{206}Tl ($\bar{p}\bar{n}$)	+1.0	-0.05
^{206}Hg (\bar{p}^2)	-2.50	-0.80
^{208}Pb ($\bar{p}\bar{p}$) and ($\bar{n}\bar{n}$)	≈ -5.0	0.0

low, the parameters α_2 and α_3 were adjusted so that the best fit to both the observed energy levels and the spectroscopic factors was obtained. ^{206}Hg is a special case and the choice of α_2 and α_3 for ^{206}Hg is discussed in more detail in Sec. III H.

Table I also includes the values of α_2 and α_3 which will give essentially the same results for ^{208}Pb as the central-plus-weak-coupling force used in TMP.

Table I indicates that the residual force consists of a fixed central Gaussian-type interaction plus P_2 and P_3 multipole interactions whose strengths are varied in order to account for model-space truncation effects which may vary from nucleus to nucleus.

III. RESULTS

In this section, the detailed results of the calculations on the eight nuclei ^{206}Pb , ^{210}Pb , ^{210}Po , ^{208}Bi , ^{210}Bi , ^{208}Tl , ^{206}Tl , and ^{206}Hg will be given. *These calculations will be referred to as MT below.*

The vector coupling scheme used in this paper is to couple \vec{l} to \vec{s} to give \vec{j} , and in the wave function $|j_1 j_2 JM\rangle$, \vec{j}_1 is coupled to \vec{j}_2 to give \vec{J} , where \vec{j}_1 and \vec{j}_2 can represent either a particle or a hole depending on the nucleus being considered.

In all cases, the calculated results have been normalized so that the ground state lies at zero energy. The calculated and experimental ground-state energies with respect to the ^{208}Pb core are compared in Table II. It should be noted that the differences between the calculated and the experimental ground-state energies in several cases are less than 100 keV and in no cases larger than 300 keV. In general, only the low-lying levels will be compared with experimental data, although in many nuclei, levels with much higher energy have also been observed. The reason for omitting the high-lying levels is in part due to the fact that the

TABLE II. Comparison of the experimental and calculated binding energies in MeV with respect to the ^{208}Pb core. The experimental binding energies were taken from J. H. E. Mattauch, W. Thiele, and A. H. Wapstra, Nucl. Phys. 67, 1 (1965). The binding energies of ^{210}Po and ^{206}Hg have been calculated using an average Coulomb energy matrix element of 0.30 MeV.

Nucleus	Binding Energy		Difference
	Exp.	Calc.	
^{206}Pb	14.11	13.90	-0.21
^{210}Pb	-9.12	-9.20	-0.08
^{210}Po	-8.78	-8.92	-0.14
^{208}Bi	3.65	3.73	0.08
^{210}Bi	-8.40	-8.58	-0.18
^{208}Tl	4.21	4.29	0.07
^{206}Tl	14.85	14.59	-0.26
^{206}Hg	15.38	15.27	-0.11

first excited 3^- state in ^{208}Pb is located at 2.6 MeV and is known to be of a collective character.¹ Since core excitations have not been explicitly taken into account in these calculations, detailed comparison of levels above 2.5 MeV may not be meaningful. That is, levels which mix strongly with collective-type core excitations are expected to be poorly described because of the limited model spaces and residual interactions used in these calculations. However, it is quite possible that some of the core-excitation effects have been accounted for by adjustment of various multipole components in the residual force.

A. Other Calculations

Some of the other calculations in the lead region with which the calculations reported in this paper will be compared will now be briefly described.

Herling and Kuo²² have calculated the level structure of several nuclei in the lead region using a Hamada-Johnston potential for the nucleon-nucleon interaction. They calculated the energy levels with: (I) the bare reaction matrix element, (II) the bare reaction matrix element renormalized by one-particle-one-hole core excitations, and (III) the bare reaction matrix element normalized by one-particle-one-hole and two-particle-two-hole core excitations. Since approximation (II) in the Herling and Kuo calculations gave the best agreement with the experimental data, we shall only compare these results with our calculations and label them as HKII below.

Hughes, Snow, and Pinkston¹⁵ have done conventional shell-model calculations in the lead region. They used a central-plus-tensor interaction with a Gaussian shape and found that in order to obtain the best fit to the experimental energies, the force parameters used for like-particle spectra (i.e., ^{206}Pb , ^{210}Pb , and ^{210}Po) should be different from those force parameters used for unlike-particle spectra (i.e., ^{208}Bi , ^{210}Bi , ^{208}Tl , and ^{206}Tl). They concluded that no single force could be found which gave a good fit to all the nuclear energy levels in the lead region. The results of their calculations will be labeled as HSP below.

Kim and Rasmussen^{9,10} used a central-plus-tensor interaction with a Gaussian shape and were able to obtain very good fits to the unlike-particle spectra of ^{208}Bi , ^{210}Bi , and ^{208}Tl . These results will be labeled as KR below.

Vary and Ginocchio²¹ used a central interaction in the random-phase approximation for the nuclei ^{206}Pb and ^{210}Pb . Their results will be labeled as VG below.

Freed and Rhodes¹⁸ have done a calculation of

the energy levels for the same eight nuclei which are discussed in this paper using a first-order Tabakin interaction plus a pairing force plus a P_2 multipole force with a single set of parameters for all eight nuclei. It appears that their results are similar to results obtained by the present authors using only the Gaussian-shaped central force given by Eq. (2). As pointed out in Sec. II, much better agreement between the observed energy levels and spectroscopic factors can be obtained by including the P_2 and P_3 multipole forces. Freed and Rhodes's results will be labeled FR below.

In addition to the calculations mentioned above, the results of a few other calculations will also be used for comparison and will be discussed in the appropriate sections below.

B. ^{206}Pb

Using the residual force described in Sec. II, the low-lying levels of ^{206}Pb which are described by two neutron holes in the ^{208}Pb core have been calculated.

These results, labeled MT, are compared with the experimental levels^{24,60} and with the calculations of True,³ Vary and Ginocchio,²¹ and Herling and Kuo²² in Fig. 2. In Fig. 2, the results labeled True were taken from the calculation by True³ who used a singlet-even Gaussian central force plus a

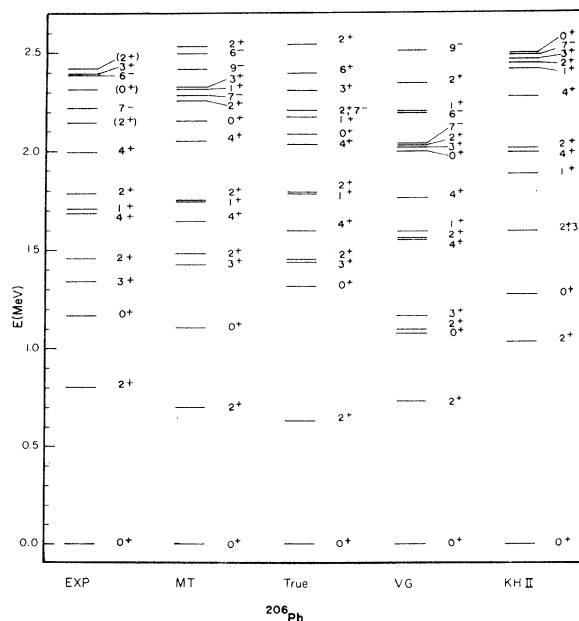


FIG. 2. Comparison of the experimentally observed energy levels (Ref. 60) of ^{206}Pb below 2.5 MeV with the calculations of MT, True, VG, and HKII.

TABLE III. Comparison between the experimental and calculated squared amplitudes of the wave functions in ^{206}Pb . The experimental data were taken from Refs. 25, 35, and 36. In Ref. 25, the $i_{13/2}^2$ amplitude was deduced by requiring the sum of the squared amplitudes to be unity.

E (MeV)	I^π		Squared amplitudes
0	0^+	Exp. (Ref. 25)	$0.54p_{1/2}^2 + 0.20f_{5/2}^2 + 0.12p_{3/2}^2 + 0.12i_{13/2}^2 + 0.03f_{7/2}^2$
		Exp. (Ref. 35)	$0.57p_{1/2}^2$
		Exp. (Ref. 36)	$0.65p_{1/2}^2 + 0.25f_{5/2}^2 + 0.20p_{3/2}^2$
		Calc.	$0.64p_{1/2}^2 + 0.16f_{5/2}^2 + 0.13p_{3/2}^2 + 0.035i_{13/2}^2 + 0.027f_{5/2}^2$
0.803	2^+	Exp. (Ref. 35)	$0.68p_{1/2}f_{5/2} + 0.22p_{1/2}p_{3/2}$
		Calc.	$0.50p_{1/2}f_{5/2} + 0.29p_{1/2}p_{3/2}$
1.17	0^+	Exp. (Ref. 35)	$0.48p_{1/2}^2$
		Exp. (Ref. 36)	$0.22p_{1/2}^2 + \leq 0.78f_{5/2}^2 + \leq 0.29p_{3/2}^2$
		Calc.	$0.30p_{1/2}^2 + 0.56f_{5/2}^2 + 0.016p_{3/2}^2$
1.34	3^+	Exp. (Ref. 35)	$1.12p_{1/2}f_{5/2}$
		Exp. (Ref. 36)	$1.00p_{1/2}f_{5/2}$
		Calc.	$1.00p_{1/2}f_{5/2}$
1.47	2^+	Exp. (Ref. 35)	$0.86p_{1/2}p_{3/2}$
		Exp. (Ref. 36)	$0.61p_{1/2}p_{3/2} + 0.39p_{1/2}f_{5/2}$
		Calc.	$0.53p_{1/2}p_{3/2} + 0.43p_{1/2}f_{5/2}$
1.71	1^+	Exp. (Ref. 35)	$1.02p_{1/2}p_{3/2}$
		Exp. (Ref. 36)	$1.00p_{1/2}p_{3/2}$
		Calc.	$1.00p_{1/2}p_{3/2}$
2.19	7^-	Exp. (Ref. 35)	$1.24p_{1/2}i_{13/2}$
		Calc.	$0.94p_{1/2}i_{13/2}$
2.38	6^-	Exp. (Ref. 35)	$0.72p_{1/2}i_{13/2}$
		Calc.	$1.00p_{1/2}i_{13/2}$
2.93	4^+	Exp. (Ref. 35)	$0.86p_{1/2}f_{7/2}$
		Calc.	$0.80p_{1/2}f_{7/2}$
3.11	(3^+)	Exp. (Ref. 35)	$1.06p_{1/2}f_{7/2}$
		Calc.	$1.00p_{1/2}f_{7/2}$

P_2 weak-coupling force. The residual force used in this paper differs essentially in that the weak-coupling force used by True has been replaced by P_2 and P_3 multipole forces with a singlet-even projection operator. It is seen that the MT calculation gives the best fit to the observed energy levels of ^{206}Pb .

In Table III, the square of the amplitudes of the wave functions are compared with those deduced from nuclear-reaction studies. In general, good agreement is obtained between the experimental data and the calculated results.

The ground-state wave function deserves special attention. Mukherjee and Cohen²⁵ reported that according to a $^{206}\text{Pb}(d,p)^{207}\text{Pb}$ reaction study, the squared amplitudes of the $p_{1/2}^2$ and $i_{13/2}^2$ neutron hole components in the ground state are 0.54 and 0.12, respectively. However, it was pointed out in their paper that the amplitude of $i_{13/2}^2$ was ob-

tained by extrapolation and hence its value is somewhat more questionable. The uncertainty in the $i_{13/2}^2$ component will also affect the other components, since the sum of the squared amplitudes is normalized to 1. Subsequent measurements all showed a somewhat larger value for the $p_{1/2}^2$ component. For example, Tickle and Bardwick³⁵ obtained the squared amplitude of the $p_{1/2}^2$ component to be 0.57 from a $^{207}\text{Pb}(d,t)^{206}\text{Pb}$ study while Richard *et al.*³⁶ obtained an even larger value of 0.65 from a $^{206}\text{Pb}(p,p')^{206}\text{Pb}$ study. The calculated squared amplitude of the $p_{1/2}^2$ component is 0.64 which agrees very well with the measurement of Richard *et al.*³⁶ The calculated squared amplitudes of the $p_{1/2}^2$ component in the three calculations of True, VG, and HKII are 0.68, 0.77, and 0.43, respectively, indicating that VG does not appear to have enough configuration mixing while HKII appears to have too much configuration mix-

TABLE IV. Comparison between the experimental and calculated $E2$ and $M1$ transition rates and branching ratios in ^{206}Pb below 2.5 MeV. The experimental data were taken from Ref. 60.

$J_i^\pi \rightarrow J_f^\pi$		Experiment		This calculation	
		T (10^{11} sec^{-1})	Branching ratio	T (10^{11} sec^{-1})	Branching ratio
2_1^+	0_1^+	1.1	100 $E2$	1.0	100 $E2$
3_1^+	2_1^+		100 $M1$	0.22	100 $M1$
2_2^+	0_1^+		(100)	3.0	4 $E2$
	2_1^+				96 $M1$
	3_1^+				0.4 $M1$
4_1^+	2_1^+		69 $E2$	3.2	56 $E2$
	3_1^+		31 $M1$		44 $M1$
	2_2^+		...		0.
4_2^+	2_1^+		10 $E2$	15	3 $E2$
	3_1^+		70 $M1$		84 $M1$
	2_2^+		(3)		0.1 $E2$
	4_1^+		17 $M1$		12 $M1$
6_1^-	7_1^-	0.24	100 $M1$	0.22	100 $M1$

ing.

It should be pointed out that a slightly better agreement for the energy levels could be obtained if the present strength of the P_3 force used in the ^{206}Pb calculation were reduced by 40%, i.e., $\alpha_3 = -3.0 \times 10^{-5} \text{ MeV/fm}^6$. This interaction, however, gives a squared amplitude of the $p_{1/2}^2$ component in the ground-state wave function of 0.68 which appears to be slightly too large. Therefore, a strength of $\alpha_3 = -5.0 \times 10^{-5} \text{ MeV/fm}^6$ was adopted which gives the best over-all agreement of the energy levels and of the ground-state wave function.

Recently, detailed γ -decay properties of the excited states in ^{206}Pb were reported by Manthuruthil *et al.*⁶⁰ Table IV compares the calculated transition rate and branching ratio with the available experimental data. $E2$ and $M1$ transitions have been restricted to those levels with energy below 2.5 MeV where a neutron effective charge of $0.87e$ was used. This effective charge fits the experimental value given by True and Ford² of the transition rate from the first 2^+ state to the ground state. Manthuruthil *et al.* tentatively give the branching ratio from the 2_2^+ level as being 100% to the 0_1^+ level. However, True and Ford² give an experimental branching ratio of $172(M1)/1(E2)$ for the 2_2^+ to $2_1^+/2_2^+$ to 0_1^+ ratio which is essentially in agreement with the calculated results given in Table IV. The Schmidt values have been used for the magnetic g_l and g_s factors in calculating the $M1$ transitions. It is seen from Table IV that there is generally good agreement between the calculated and experimental results. The calculated and experimental $M1$ transition rate from the first 6^- state to the 7^- state are $0.22 \times 10^{11}/\text{sec}$ and $0.24 \times 10^{11} \text{ sec}$, respectively. This excellent agreement is probably accidental, since the effective g_l and g_s factors in the present model space will

probably be different from the Schmidt values.⁵⁷ Therefore, one would expect these calculations to give only qualitative agreement as far as the $M1$ transitions are concerned. Manthuruthil *et al.*⁶⁰ also reported the calculated transition rates and branching ratios using the different wave function sets of True, VG, and HKII for levels up to 3.3 MeV. In general, the results on branching ratios in this paper are similar to those of True, although the transition rates in some cases differ by 20%.

Manthuruthil *et al.* have also observed $E1$ transitions between some of the high-lying states. For example, they observed $E1$ transitions from the $J = 5^-$ state at 2.78 MeV to the $J = 4^+$ states at 1.68 and 2.00 MeV, from the 2.83-MeV $J = 4^-$ state to the 1.68-MeV $J = 4^+$ state, and from the 3.02-MeV $J = 5^-$ state to the 1.68-MeV $J = 4^+$ state while $E1$ transitions are forbidden in our model space. In addition, Manthuruthil *et al.* have observed five $J = 5^-$ states while our model space can produce only four $J = 5^-$ states. These aspects suggest the need of enlarging the present model space in order to account for the properties of the higher-lying levels.

C. ^{210}Pb

The structure of ^{210}Pb which is described by two neutron particles outside the ^{208}Pb core has been

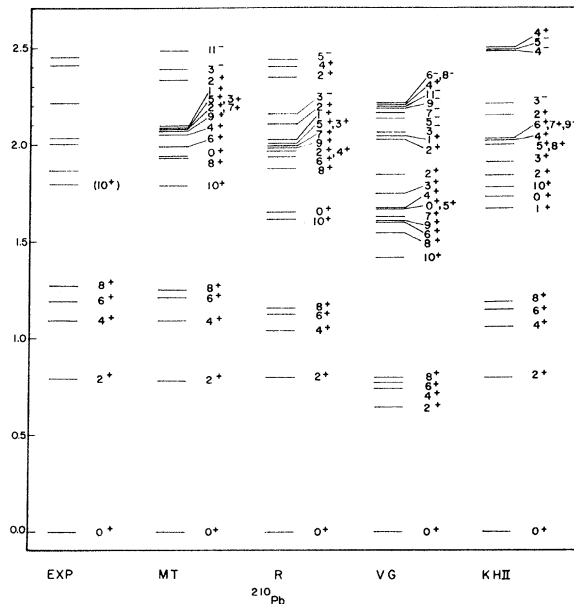


FIG. 3. Comparison of the experimentally observed energy levels (Ref. 61) of ^{210}Pb below 2.5 MeV with the calculations of MT, R, VG, and HKII.

calculated using the residual force described in Sec. II.

Figure 3 compares the experimental energy levels below 2.5 MeV with the present calculations, and with the calculated results of Redlich¹¹ (labeled by R), VG,²¹ and HKII.²² Redlich used a singlet-even Gaussian-shaped interaction with a strength about 30% stronger than V_0 . The MT calculations give the best fit with the observed levels. For the lowest five excited states below 1.8 MeV, the differences between our calculations and the experimental data are all less than 20 keV which is indeed excellent. The level at 1.87 MeV has been identified in a $^{210}\text{Pb}(t, t')$ ^{210}Pb reaction by Jardine⁵⁸ as being a $J = 3^-$ state which is lower than the $J = 3^-$ collective state in ^{208}Pb by about 700 keV. Beery,⁶⁴ on the basis of his experimental results, has tentatively assigned a spin of $J = 6^+$ or 8^+ to this state. These calculations give a $J = 3^-$ state at 2.39 MeV, a $J = 8^+$ state at 1.93 MeV and a $J = 6^+$ state at 2.00 MeV, hence these results support a $J = 6^+$ or 8^+ spin assignment for the 1.87-MeV level. For levels above 1.9 MeV there is less detailed experimental information and no detailed comparison has been made.

Recently, Igo *et al.*⁴⁶ have measured the squared amplitudes of the ground-state wave function of ^{210}Pb using the $^{210}\text{Pb}(p, d)^{209}\text{Pb}$ reaction. The comparison between their observed results and those predicted by different calculations is given in Table V. Both MT and HKII give very good agreement. A recent calculation by Freed and Rhodes¹⁸ (labeled FR) using a Tabakin interaction plus a pairing interaction plus a P_2 multipole interaction also produced a good fit to the ground-state wave function. On the other hand, both the calculations of Redlich and VG do not have enough configuration mixing and their ground-state wave functions contain too large a $g_{9/2}^2$ component as compared with the experimental data.

In the present calculations, the strength of the P_2 force is set to zero. Actually, there exist several sets of P_2 and P_3 strengths which can give

TABLE V. The comparison between the observed squared amplitudes (Ref. 46) of the neutron-particle components in the ground-state wave function of ^{210}Pb and those predicted by various calculations.

	$g_{9/2}^2$	$i_{11/2}^2$	$j_{15/2}^2$	$d_{5/2}^2$	$s_{1/2}^2$	$g_{7/2}^2$	$d_{3/2}^2$
Exp.	0.67	0.16	0.17	0.01	0.0015	0.015	0.0035
MT	0.70	0.10	0.16	0.01	0.0017	0.024	0.0031
HKII	0.68	0.17	0.09	0.02	0.0031	0.030	0.0067
FR	0.72	0.19	0.08
R	0.79	0.10	0.05	0.02	0.0045	0.026	0.0075
VG	0.86	0.09	0.04	0.01	0.0025	0.024	0.0052

equally good energy-level fits. However, the observed large squared amplitude of the $j_{15/2}^2$ component in the ground-state wave function can only be obtained in our calculations by introducing a large P_3 force while it is very insensitive to the P_2 force. Therefore, the present strengths of P_2 and P_3 forces in Table I are used in order to give good fit both to the energy levels and the ground-state wave function.

D. ^{210}Po

Recent electron-capture^{38,54,58} and nuclear-reaction^{42,49,51,53} studies have provided detailed information about the structure of the low-lying levels in ^{210}Po . The ^{210}Po levels which can be described by two proton particles outside the ^{208}Pb core were calculated using the residual force described in Sec. II and the results are compared with the available experimental data below.

Experimentally the energy levels reveal multiplet structure in ^{210}Po . It is seen from Fig. 4 that the grouping of levels, the energy spread for each multiplet, and the gap between different multiplets are all well reproduced by calculations of MT and HKII.²² The calculation of Freed and Rhodes,¹⁸ labeled FR, does not give as good a fit to the energy spectra. MT gives a better agree-

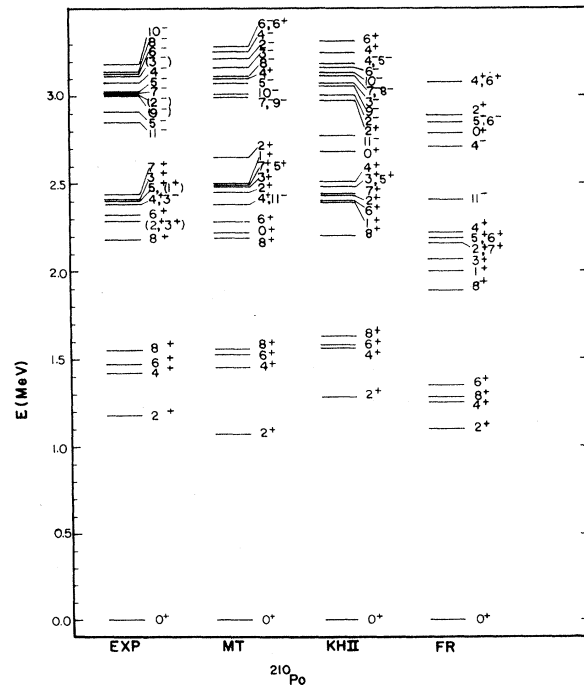


FIG. 4. Comparison of the experimentally observed energy levels (Ref. 54) of ^{210}Po below 3.2 MeV with the calculations of MT, HKII, and FR.

ment for the lowest $h_{9/2}^2$ multiplet while HKII does better for the $h_{9/2} i_{13/2}$ multiplet located at about 3 MeV. Both calculations give similar fits to the $h_{9/2} f_{7/2}$ multiplet located at about 2.3 MeV. Figure 4 also gives the calculated even-parity states of the $f_{7/2}^2$ multiplet whose levels with spins of 0^+ , 2^+ , 4^+ , and 6^+ spread from 2.22 to 3.28 MeV in the MT calculation and spread from 2.68 to 3.3 MeV in the calculation of HKII. Unfortunately there is not enough experimental data at this time for a more detailed comparison.

Figure 4 indicates that the model space is not large enough to include all the observed low-lying negative-parity states. For example, the two observed $J = 3^-$ states at 2.39 and 3.11 MeV arise most probably from the coupling between the $J = 3^-$ core state and the $h_{9/2} i_{13/2}$ $J = 3^-$ multiplet component. Similarly the two observed $J = 5^-$ states at 2.91 and 3.03 MeV most probably come from the coupling between the first $J = 5^-$ core state and the $h_{9/2} i_{13/2}$ $J = 5^-$ multiplet component. Since the model space contains only the $h_{9/2} i_{13/2}$ configuration and does not explicitly include the particle-hole excitations of the core, only one $J = 3^-$ state and one $J = 5^-$ state appear in this energy region. The calculated $J = 3^-$ and $J = 5^-$ states agree very well with the observed second $J = 3^-$ and second

$J = 5^-$ states. Thus it seems that the lowest observed $J = 3^-$ and $J = 5^-$ are predominantly core excitations. The calculated $J = 11^-$ state of MT is much too low compared with the observed one and it is not understood why.

Kim and Rasmussen⁹ have also calculated ^{210}Po using the same force as they used in ^{210}Bi , ^{208}Bi , and ^{208}Tl . In their calculations, the off-diagonal matrix elements of the tensor force were neglected and a good fit was obtained. HSP pointed out, however, that the results of Kim and Rasmussen in ^{210}Po will become considerably worse if the off-diagonal matrix elements of the tensor force are included.

One would like to point out here that the Coulomb force has not been taken into account in the present calculations. Including the Coulomb force will depress the energy levels in general. The changes, however, can for the most part be compensated for by readjustment of the strengths of the P_2 and P_3 forces. For example, a calculation which includes Coulomb force and which uses a new value of $\alpha_3 = -1.35 \times 10^{-4}$ MeV fm⁶ (compared with the present value of $\alpha_3 = -1.20 \times 10^{-4}$ MeV/fm⁶) gives essentially the same energies and wave functions as the present calculation.

The spectroscopic factors in ^{210}Po have been

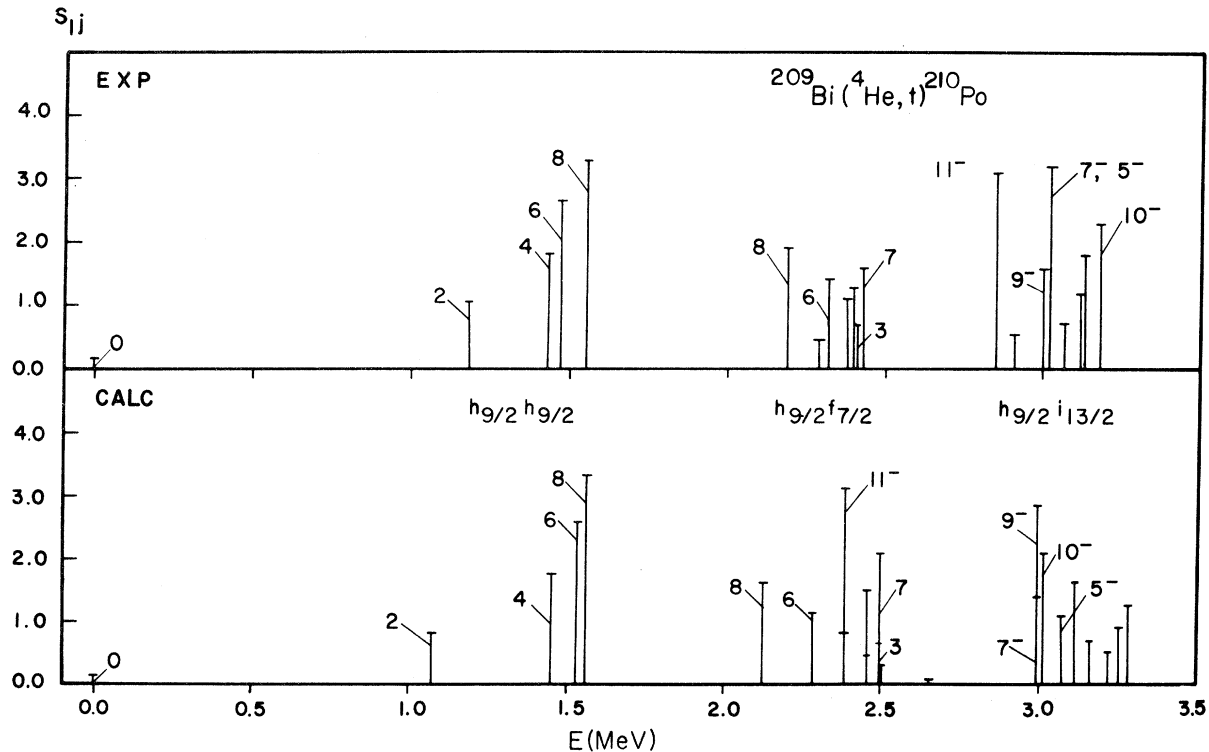


FIG. 5. Comparison of the experimentally observed spectroscopic factors (Ref. 53) from the $^{209}\text{Bi}(\alpha, t)^{210}\text{Po}$ reaction with the calculated values. The spins of some of the more prominent spectroscopic factors are indicated and have positive parity unless otherwise indicated. Whenever a calculated doublet occurs, the total line represents the sum of the two spectroscopic factors with a bar part way up the line indicating the division of the individual strengths.

studied by Lanford, Alford, and Fulbright⁵³ using $^{209}\text{Bi}(\text{He}^4, t)^{210}\text{Po}$ and $^{209}\text{Bi}(\text{He}^3, d)^{210}\text{Po}$ reactions. They found that the low-lying states in general have very pure multiplet configurations. This pure multiplet structure is also present in these calculations—except for the $J=0^+$ ground state whose wave function contains configuration mixing of the $h_{9/2}^2$, $f_{7/2}^2$, and $i_{13/2}^2$ components. Figure 5 compares the calculated stripping spectroscopic factor S_{lj} of the $|h_{9/2}, lj, J\rangle$ components with those observed by Lanford, Alford, and Fulbright.⁵³ The spectroscopic factor S_{lj} is defined as

$$S_{lj} = (2J+1) a_{lj}^2 / (2I+1), \quad (4)$$

where J is the spin of the ^{210}Po excited states, $I = \frac{9}{2}$ is the spin of the ^{209}Bi ground state, and a_{lj} is the amplitude of the $|h_{9/2}, lj, J\rangle$ component in the wave function. However, in the special case of $lj = h_{9/2}$, the S_{lj} is defined as

$$S_{lj} = 2(2J+1) a_{lj}^2 / (2I+1), \quad (5)$$

where the additional normalization constant 2 is introduced to satisfy the sum rule,⁷⁰ i.e., the sum of the spectroscopic factor S_{lj} over all states should be equal to the number of proton holes in the l, j orbital. It is seen from Fig. 5 that the predicted results agree quite well with the experimental data.

Jardine, Prussin, and Hollander⁵⁴ and Jardine⁵⁸ have studied the electron-capture decay of ^{210}At and observed many γ transitions between the energy levels in ^{210}Po . Their results on the transition rates, branching ratios, and the $E2$ - $M1$ mixing ratios are compared with the calculated results in Table VI. In these calculations, the proton effective charge is chosen to be $e_{\text{eff}} = 1.5e$ and the magnetic g_i and g_s factors are chosen to have the Schmidt values. It is seen in Table VI that the predicted $E2$ transition rates of the $h_{9/2}^2$ multiplet agree very well with the experimental data. The agreement on the branching ratios is in general also good. The observed $E1$ - $M1$ mixing ratios are poorer in this case. Nevertheless, they are consistent with these calculations for the most part. As was pointed out in the discussion of ^{208}Pb above, in order to have a better fit to the branching ratios and the $E2$ - $M1$ mixing ratios, one probably has to use effective g_1 and g_s values rather than the Schmidt values.⁵⁷

E. ^{208}Bi

Up to this point, the like-particle spectra of ^{206}Pb , ^{210}Pb , and ^{210}Po have been considered. Now the unlike-particle spectra of ^{208}Bi , ^{210}Bi , ^{208}Tl , and ^{206}Tl will be considered. ^{208}Bi will be described by one proton particle outside and one neutron hole in the ^{208}Pb core and $j_1 \bar{j}_2$ will represent a proton

TABLE VI. Comparison between the experimental (Refs. 54 and 58) and calculated transition rates, branching ratios, and $E2$ - $M1$ mixing ratios in ^{210}Po . The $E2$ - $M1$ mixing ratio is defined as $T(E2)/T(M1)$.

J_i^{π}	J_f^{π}	Experiment			This calculation		
		T (sec^{-1})	Branching ratio	$E2$ - $M1$ mixing ratio	T (sec^{-1})	Branching ratio	$E2$ - $M1$ mixing ratio
2_1^+	0_1^+	...			8.34×10^{11}	100 $E2$	
4_1^+	2_1^+	$(3.3 \pm 0.4) \times 10^8$	100 $E2$		3.43×10^8	100 $E2$	
6_1^+	4_1^+	$(6.7 \pm 0.9) \times 10^4$	100 $E2$		6.06×10^4	100 $E2$	
8_1^+	6_1^+	$(3.7 \pm 0.3) \times 10^5$	100 $E2$		4.47×10^5	100 $E2$	
7_1^+	8_1^+		35 $M1 + E2$	$0.58^{+0.47}_{-0.29}$	3.23×10^{11}	38 $M1 + E2$	0.051
	8_2^+		34 $M1$	<0.32		50 $M1$	3.0×10^{-5}
	6_1^+		26 ...			6 $M1 + E2$	
	6_2^+		~5 $M1$			6 $M1$	
5_1^+	6_1^+		47 $M1$	<0.32	1.21×10^{11}	57 $M1$	7.7×10^{-3}
	6_2^+		2 ($M1$)			11 $M1$	
	4_1^+		51 ($M1$)	<0.19		32 $M1 + E2$	0.23
8_2^+	8_1^+		88 $M1$	<0.19	2.87×10^{11}	100 $M1$	6.1×10^{-3}
	6_1^+		<12 ...			2×10^{-6} $E2$	
6_2^+	8_1^+		<3 ...		6.73×10^{10}	0.2 $E2$	
	6_1^+		85 $M1$	$0.19^{+1.6}_{-0.14}$		95 $M1 + E2$	0.20
	4_1^+		<12 ...			5 $E2$	
4_2^+	6_1^+		4 ...		2.75×10^{11}	3 $E2$	
	4_1^+		88 $M1$	<0.29		78 $M1 + E2$	0.076
	2_1^+		8 ($E2$)			20 $E2$	
	2_2^+		~0.04 ($E2$)			9×10^{-4} $E2$	

particle j_1 coupled to a neutron hole j_2 .

The experimental information on the structure of the ^{208}Bi levels has been determined mainly by nuclear reactions^{29,47} and nuclear decay^{40,41,43} studies. The detailed analysis by Alford, Schiffer, and Schwartz⁴⁷ indicates that the levels below 3.0 MeV which are strongly excited by the proton stripping reactions $^{207}\text{Pb}(\alpha, t)^{208}\text{Bi}$ and $^{207}\text{Pb}(\text{He}^3, d)^{208}\text{Bi}$ or by the neutron pickup reactions $^{209}\text{Bi}(d, t)^{208}\text{Bi}$ and $^{209}\text{Bi}(\text{He}^3, \alpha)^{208}\text{Bi}$ form doublets and multiplets arising either from an lj proton particle coupled to a $p_{1/2}$ neutron hole or from a $h_{9/2}$ proton particle coupled to an lj neutron hole. The experimental energies are compared with those calculated by MT, KR,¹⁰ and Kuo¹⁶ in Fig. 6. It is seen in Fig. 6 that except for the $h_{9/2}\bar{f}_{7/2}$ and $h_{9/2}\bar{i}_{13/2}$ multiplets, the agreements are very good for the calculations of MT and KR. Kuo's calculation is also good except the energy spread of the $h_{9/2}\bar{f}_{5/2}$ multiplet is somewhat larger. KR and Kuo obtained good agreement for the $h_{9/2}\bar{f}_{7/2}$ multiplet, while the MT results are not as good. For the $h_{9/2}\bar{i}_{13/2}$ multiplet, none of the three calculations yield satisfactory results. It is possible in this energy region that the coupling to the core excitations could become important, and hence a larger model space with explicit corrections for core excitation is needed. It was also mentioned in Ref.

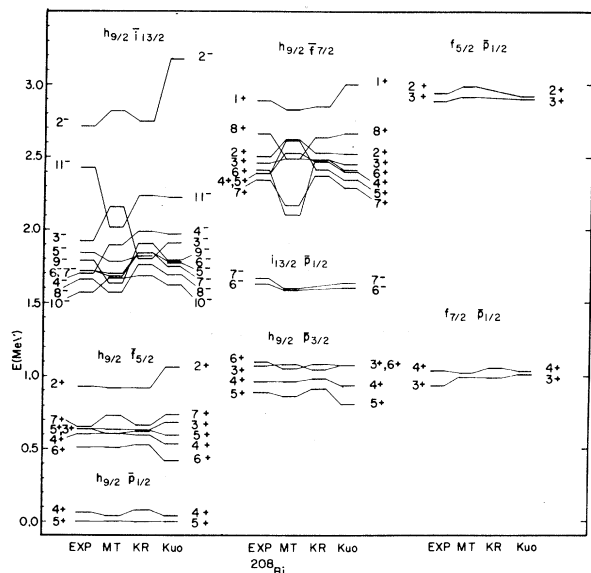


FIG. 6. Comparison of the experimentally observed multiplets (Ref. 47) of ^{208}Bi with the calculations of MT, KR, and Kuo. Only those calculated levels with a dominant multiplet component are shown with the remaining multiplet strength being distributed among other levels which may or may not appear in the figure.

47 that their spin assignments are not uniquely determined from the reaction cross sections and an uncertainty of perhaps ± 1 should be assigned to the values of the spin I assigned to the levels in this energy region.

For energies above 3.0 MeV, additional multiplets belonging to the $h_{9/2}\bar{h}_{9/2}$, $p_{3/2}\bar{p}_{3/2}$, and $p_{1/2}\bar{p}_{1/2}$ configurations were also observed by the authors of Ref. 47 but they did not determine the spins of these multiplets. Recently, Crawley *et al.*⁵² have tentatively given energies and spins to the $h_{9/2}\bar{h}_{9/2}$ multiplet. These experimental results are compared with these calculations in Table VII. As can be seen by Table VII, the lower spin states, 0^+ to 3^+ , are less pure and for a given spin, the calculated state with the second largest $h_{9/2}\bar{h}_{9/2}$ component usually agrees best with the experimental energies. It is not understood why these other states with larger $h_{9/2}\bar{h}_{9/2}$ amplitudes were not seen unless the experiment was restricted to a certain energy region and/or these states have been mislabeled. On the other hand, the higher spin states, 4^+ to 9^+ , are generally more pure and the calculated state with the largest $h_{9/2}\bar{h}_{9/2}$ component agrees quite well with the experimental energies.

The spectroscopic factors of ^{208}Bi have also been measured.⁴⁷ Their results indicated that the observed states below 3.0 MeV are in general described by very pure multiplets. This "purity" is also confirmed in general by these calculations. Figure 7 shows the spectroscopic factors distribution below 4.0 MeV. Figure 7(a) gives the spectroscopic factors S_{ij} obtained from the $^{207}\text{Pb}(\text{He}^3, d)$ -

TABLE VII. The comparison between the experimental (Ref. 52) and the calculated energies in MeV of the states of the $h_{9/2}\bar{h}_{9/2}$ multiplet in ^{208}Bi . The number in parentheses after the calculated energy represents the amplitude of the $h_{9/2}\bar{h}_{9/2}$ component for that level. The 1^+ , 3^+ and 5^+ , 7^+ doublets were not experimentally resolved.

J^π	Experiment	This calculation
0^+	3.896	1.03 (0.22) 3.88 (0.14) 4.72 (0.83)
1^+	3.371	3.62 (-0.33) 4.12 (0.55)
2^+	3.550	3.53 (-0.34) 3.99 (0.80)
3^+	3.371	3.44 (0.45) 3.88 (0.71)
4^+	3.533	3.64 (0.90)
5^+	3.421	3.46 (0.76)
6^+	3.281	3.53 (0.98)
7^+	3.421	3.51 (0.89)
8^+	3.473	3.45 (0.99)
9^+	3.574	3.75 (1.00)

^{208}Bi stripping reaction where S_{ij} is defined by Eq. (4) with $I = \frac{1}{2}$ for the spin of the ground state of ^{207}Pb . Figures 7(b) and 7(c) give the spectroscopic factors, S_{ij} , obtained from the $^{208}\text{Bi}(d,t)$ - ^{208}Bi pickup reactions where S_{ij} is defined by Eq. (4). Comparisons of the experimental and the calculated results in Fig. 7 indicate that the agreements are generally good. The general features like the occurrence of doublets and multiplets, their locations, the separations between different multiplets, and the strength distribution are all reasonably well reproduced. On the other hand, one notes that the calculated strengths of the $h_{9/2} \bar{f}_{13/2}$ and $h_{9/2} \bar{f}_{7/2}$ multiplets are slightly more fragmented than the experimentally observed strengths, and that above 3.0 MeV the agreement is less good.

In addition to the multiplets which are dominated by the proton-particle and neutron-hole components of $h_{9/2} \bar{f}_n$ or $j_p \bar{p}_{1/2}$, the proton stripping reaction on ^{207}Pb and the neutron pickup reaction on ^{208}Bi can also weakly excite states which belong to other multiplets which contain small amounts of the $h_{9/2} \bar{f}_n$ or $j_p \bar{p}_{1/2}$ configurations. The spectroscopic factors of the weakly excited states thus provide a test of the configuration mixing of the small components. The experimental spectroscopic factors of the weakly excited states obtained in Ref. 47 are compared with the calculated values in Table VIII. It is seen from Table VIII that the experimental spectroscopic factors for the stripping reaction $^{207}\text{Pb}(^3\text{He}, d)^{208}\text{Bi}$ are in general larger than the calculated ones. Hence the observed data indicate a somewhat larger configuration mixing for the smaller components under consideration than the calculations give. In addition to those states listed in Table VIII, Ref. 47 also mentions other weakly excited states whose spins have not yet been determined and detailed comparison for these states will not be given.

TMP discussed in Sec. IV the position and structure of the isobaric analog of the ^{208}Pb ground state which is a high-lying excited $J = 0^+$ state in ^{208}Bi . The present calculation differs in that the weak-coupling force used in TMP is now replaced by a P_3 multipole force with singlet-even and triplet-even projection operators. With the residual force discussed in Sec. II, the analog state was calculated to be at 18.8 MeV which is close to the observed value of 18 MeV,⁵⁹ while in TMP the analog state was calculated to be at 17.2 MeV. The squared amplitudes of the particle-hole components of the calculated 18.8-MeV $J = 0^+$ state and those of a pure analog state are given in Table IX where the results of TMP are also included for comparison. For a more detailed discussion of this analog state, see TMP, Sec. IV.

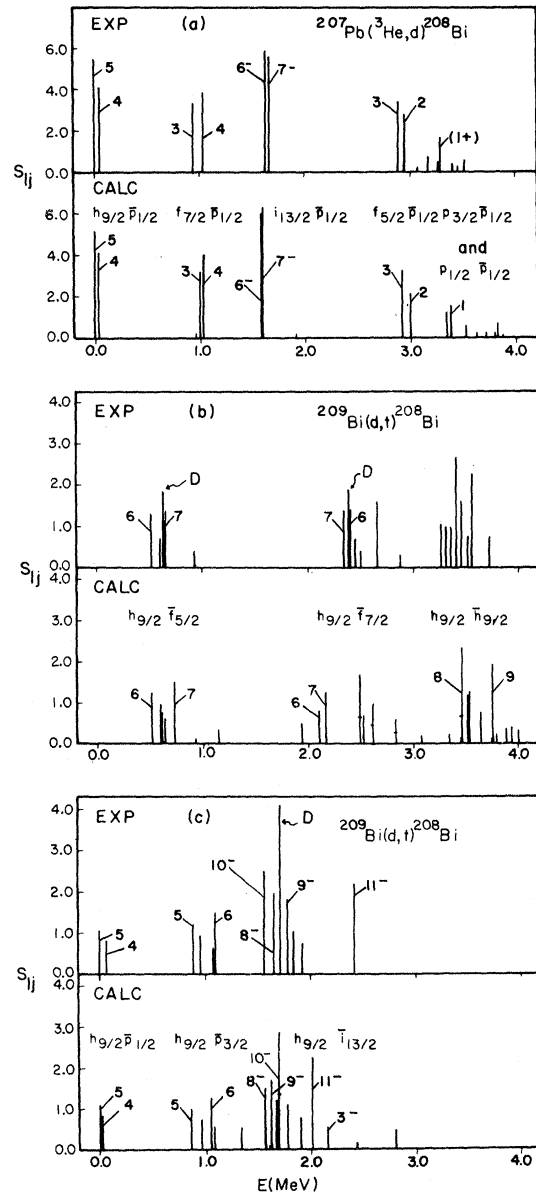


FIG. 7. Comparison of the experimentally observed spectroscopic factors from the $^{207}\text{Pb}(^3\text{He}, d)^{208}\text{Bi}$ and $^{209}\text{Bi}(d, t)^{208}\text{Bi}$ reactions (Ref. 47) with the calculated values. The spins of some of the more prominent spectroscopic factors are indicated and have positive parity unless otherwise indicated. Some experimental levels do not have a spin assigned to them, and D represents an experimental doublet. Whenever a calculated doublet occurs, the total line represents the sum of the two spectroscopic factors with a bar part way up the line indicating the division of the individual strengths. Since the multiplet strength is often distributed among several calculated levels, lines will appear here for levels which are not shown in Fig. 6.

TABLE VIII. The comparison between the experimental (Ref. 47) and calculated spectroscopic factors of the weakly excited states in ^{208}Bi . The spectroscopic factors for the strongly excited states are depicted in Fig. 7. The assignments in parentheses are based on our calculations only. The 1.719-MeV level is a doublet and S_{calc} is the sum of the spectroscopic factors for these two levels.

J^π	E_{exp} (MeV)	E_{calc} (MeV)	$^{209}\text{Bi}(d,t)^{208}\text{Bi}$			$^{207}\text{Pb}(\text{He}^3,d)^{208}\text{Bi}$			Dominant component $p\bar{n}$
			l	S_{exp}	S_{calc}	l	S_{exp}	S_{calc}	
4 ⁺	0.603	0.606	1	0.10	0.11	5	0.76	0.13	$h_{9/2}\bar{f}_{5/2}$
5 ⁺	0.631	0.603	3	0.70	0.77	or 3	0.09	0.03	$h_{9/2}\bar{f}_{5/2}$
4 ⁺	1.038	1.026	1	0.11	0.006		Strongly excited		$f_{7/2}\bar{p}_{1/2}$
(5 ⁺)	1.467	1.461	3	0.005	0.005				$(f_{7/2}\bar{f}_{5/2})$
6 ⁻	1.630	1.586	6	0.1	0.04		Strongly excited		$i_{13/2}\bar{p}_{1/2}$
6 ⁻ } 7 ⁻ }	1.719	{1.684} {1.701}		Strongly excited		6	2.1	0.7	$h_{9/2}\bar{i}_{13/2}$
3 ⁺	2.462	2.491		Strongly excited		3	0.17	0.06	$h_{9/2}\bar{f}_{7/2}$
2 ⁺	2.506	2.623		Strongly excited		3	0.11	0.07	$h_{9/2}\bar{f}_{7/2}$

Finally, it can be pointed out that a pure Gaussian force is able to give a very good fit for the levels below 1.5 MeV—the only exception is the first $J = 2^+$ state which is 140 keV too high. A P_2 force will push the $J = 2^+$ state even higher. The P_3 force, however, will depress the $J = 2^+$ state while leaving all the other levels essentially unchanged. The best fit for levels below 1.5 MeV is obtained by using only the P_3 force with the strength given in Table I.

F. ^{210}Bi

The energy levels of ^{210}Bi described by a proton particle and a neutron particle outside the ^{208}Pb core were calculated using the residual force described in Sec. II.

^{210}Bi has a ground-state spin of $J = 1^-$ which is an exception to Nordheim's strong rule for odd-odd nuclei. Shell-model calculations using "reasonable" residual forces usually produce a $J = 0^-$ level below the lowest $J = 1^-$ level. If the energy levels of ^{210}Bi are calculated using the Gaussian residual

force described in Sec. II without the P_2 and P_3 multipole forces, the calculated energy levels agree quite well with the observed levels except that the lowest $J = 0^-$ level lies 210 keV below the lowest $J = 1^-$ level. P_2 and P_3 multipole forces of varying strengths were next added to this Gaussian force in an attempt to invert the ordering of the lowest $J = 0^-$ and $J = 1^-$ levels without destroying the reasonably good fit to the higher-energy levels. A negative P_3 multipole force will raise the $J = 0^-$ level relative to the $J = 1^-$ level, while a negative P_2 multipole force has very little effect on the relative spacing of these two levels. However, both the negative P_2 and P_3 multipole forces will cause the other energy levels belonging to the $h_{9/2}g_{9/2}$ multiplet to move upward and destroy the previous good energy-level agreement. A positive P_2 multipole force, on the other hand, will tend to depress the energy of the excited states and leave the $J = 0^-$ and $J = 1^-$ spacing essentially unchanged. The best fit to the energy levels was obtained by using the positive P_2 and the negative P_3 multipole

TABLE IX. Comparison between the squared amplitudes of the calculated 18.8-MeV 0^+ state in ^{208}Bi and those of a pure isobaric-analog state. T is the isospin of the ^{208}Pb ground state. The results labeled TMP are from True, Ma, and Pinkston (Ref. 1).

$ j_p\bar{j}_n\rangle$	$i_{13/2}\bar{i}_{13/2}$	$f_{5/2}\bar{f}_{5/2}$	$h_{9/2}\bar{h}_{9/2}$	$f_{7/2}\bar{f}_{7/2}$	$p_{3/2}\bar{p}_{3/2}$	$p_{1/2}\bar{p}_{1/2}$
This calc.	0.35	0.12	0.19	0.25	0.07	0.03
TMP calc.	0.26	0.15	0.24	0.19	0.12	0.05
$\frac{2j+1}{2T}$	0.32	0.14	0.23	0.18	0.09	0.05

forces given in Table I. The calculated energy levels are compared with the experimental levels and the calculations of KR⁹ and HKII²² in Fig. 8.

The lowest calculated $J = 0^-$ level is 81 keV below the lowest $J = 1^-$ level while experimentally it is observed to be 47 keV higher. Considering the approximations made in the calculations described in this paper, this single discrepancy of 128 keV does not seem unreasonable since most of the low-lying levels of the nuclei described in this paper are fitted to within a range of 50 to 100 keV or less. However, there are usually a few levels in each nuclei in which the difference between the calculated and experimentally observed energies exceeds 100 keV. The relative position of the $J = 0^-$ level with respect to the $J = 1^-$ level could be improved by adjustment of the P_2 and P_3 multipole strengths providing a slightly poor fit to the higher-energy levels is acceptable.

KR,⁹ however, were able to explain correctly the ordering of the $J = 0^-$ and $J = 1^-$ levels in ²¹⁰Bi by introducing a tensor force. Their calculations

indicate that the position of the $J = 0^-$ level relative to the $J = 1^-$ level depends rather sensitively on the parameters of the tensor force, and hence one has to be very careful in choosing the parameters. Later, HSP¹⁵ were also able to explain the relative spacing of the $J = 0^-$ and $J = 1^-$ states by using a carefully chosen tensor force even though their force parameters were quite different from those of KR. On the other hand, recent calculations using realistic forces such as those of HKII and of FG¹⁹ still fail to produce the correct position of the $J = 0^-$ state even though both calculations included tensor forces. For example, HKII found the $J = 0^-$ state to be 70 keV below the $J = 1^-$ state, which is similar to our result, while FG found the $J = 0^-$ state to be about 200 keV below the $J = 1^-$ state. The results of these authors may indicate that either the tensor force was not treated properly, or that the inversion of the $J = 0^-$ and $J = 1^-$ spin states is actually due to some other reason(s). For example, these calculations show that the position of the $J = 0^-$ state depends strongly on the P_3

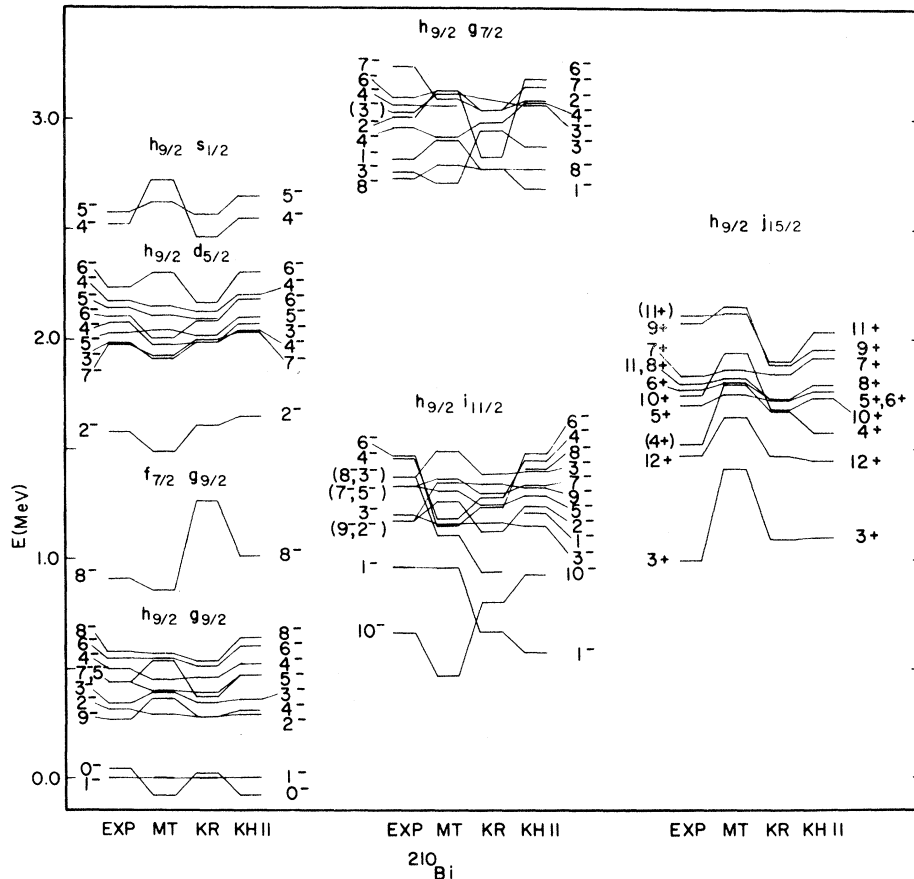


FIG. 8. Comparison of the experimentally observed multiplets in ²¹⁰Bi (Ref. 66) with the calculations of MT, KR, and HKII. Only those calculated levels with a dominant multiplet component are shown with the remaining multiplet strength being distributed among other levels which may or may not appear in the figure.

multipole force. Hence a calculation which explicitly considers the core excitations responsible for the lowest collective $J=3^-$ state on ^{208}Pb may have a large effect on the relative position of the $J=0^-$ level.

The structure of higher excited states in ^{210}Bi will now be discussed. Recent nuclear reaction^{26,65,66} and nuclear decay^{48,62} studies demonstrate that many of the levels in ^{210}Bi may be grouped into multiplets. The experimental results of Cline *et al.*⁶⁶ are compared with those calculated by MT, KR, and HKII in Fig. 8. It is seen

from Fig. 8 that the clusters of levels are well reproduced by all calculations. The degree of detailed agreement for individual levels are in general also good, although the agreement varies for different multiplets and for different calculations. For example, most of the calculated levels belonging to the $h_{9/2}g_{9/2}$, $h_{9/2}d_{5/2}$, $h_{9/2}s_{1/2}$, and $h_{9/2}g_{7/2}$ multiplets agree with the experimental data to within 100 keV, while the agreements of the $h_{9/2}i_{11/2}$ and $h_{9/2}j_{15/2}$ multiplets are less satisfactory. On the other hand, the experimental spin assignments and multiplet classification in some

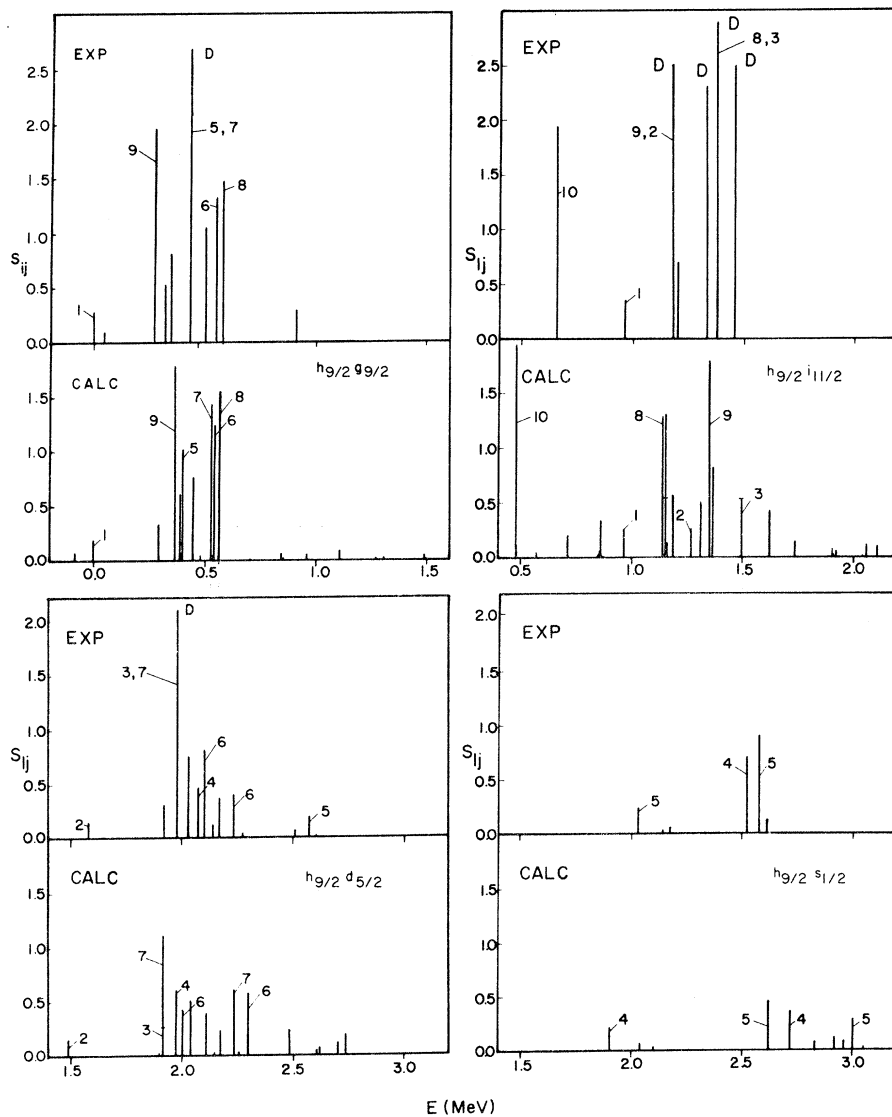


FIG. 9. Comparison of the experimentally observed spectroscopic factors in ^{210}Bi (Ref. 66) with the calculated values. The spins of some of the more prominent spectroscopic factors are indicated. Some experimental levels do not have a spin assigned to them, and D represents an experimental doublet. Since the multiplet strength is often distributed among several calculated levels, lines will appear here for levels which are not shown in Fig. 8.

cases are not well established, and hence the comparison between the experimental and calculated levels is only tentative. Consequently, it is hard to tell which calculation gives the best over-all fit to ^{210}Bi . The calculations indicate that, except for the $J=1^-$ ground state, all members of the $h_{9/2}g_{9/2}$ and $h_{9/2}j_{15/2}$ multiplets contain very pure configurations while the other multiplets involve appreciable configuration mixing. Figures 9 and 10 compare the experimental spectroscopic factors obtained from the $^{209}\text{Bi}(d,p)^{210}\text{Bi}$ reaction^{65,66} with the calculated results where S_{ij} is defined by Eq. (4). The agreement is in general good. The calculated spectroscopic strengths are more fragmented than the experimental data for the $h_{9/2}i_{11/2}$ and $h_{9/2}s_{1/2}$ multiplets. Figure 10 displays the results of the two different experimental measurements by Kolata and Daehnick⁶⁵ and by Cline *et al.*⁶⁶ The two sets of data are quite different from each other and the calculated results seem to agree better with the average of these two experiments than with any one particular experiment.

G. ^{208}Tl

^{208}Tl will be described by one neutron particle outside and one proton hole in the ^{208}Pb core.

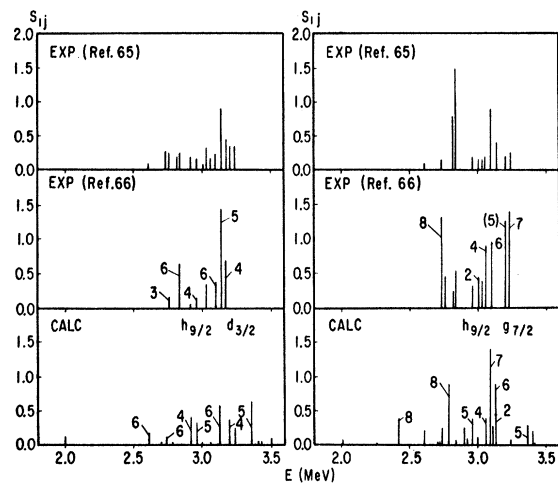


FIG. 10. Comparison of the experimentally observed spectroscopic factors from the $^{209}\text{Bi}(d,p)^{210}\text{Bi}$ reaction (Refs. 65 and 66) with the calculated values for the $h_{9/2}d_{3/2}$ and $h_{9/2}g_{7/2}$ multiplets. The spins of some of the more prominent spectroscopic factors are indicated—Ref. 65 did not assign spin values. Whenever a calculated doublet occurs, the total line represents the sum of the two spectroscopic factors with a bar part way up the line indicating the division of the individual strengths. Since the multiplet strength is often distributed among several calculated levels, lines will appear here for the multiplets which correspond to levels which are not shown in Fig. 8.

Eight levels in ^{208}Tl were observed^{28,32,63} from the α decay of ^{212}Bi . Figure 11 compares the experimental energy levels below 1.0 MeV with those calculated by MT, KR,¹⁰ and HSP.¹⁵ Both KR and HSP included tensor force in their calculations, and, in addition, they also used a smaller model space. That is, HSP considered only the lowest three proton-hole orbits, $s_{1/2}$, $d_{3/2}$, and $h_{11/2}$, while KR considered only the lowest two proton-hole orbits, $s_{1/2}$ and $d_{3/2}$. Calculations show that the first $J=2^+$ and $J=3^+$ levels contain large admixtures of the $g_{9/2}d_{5/2}$ configuration and the use of such small model spaces by KR and HSP is probably the reason why they failed to reproduce the observed narrow spacing between the first $J=3^+$ and second $J=4^+$ levels. Due to the lack of experimental information on the structure of the energy levels in ^{208}Tl , a more detailed comparison between theory and experiment is not feasible at the present time.

H. ^{206}Tl

The energy levels in ^{206}Tl which are described by a proton hole and a neutron hole in the ^{208}Pb core have been calculated with the residual force described in Sec. II. The calculated energies are compared with the experimental levels^{31,44} and the

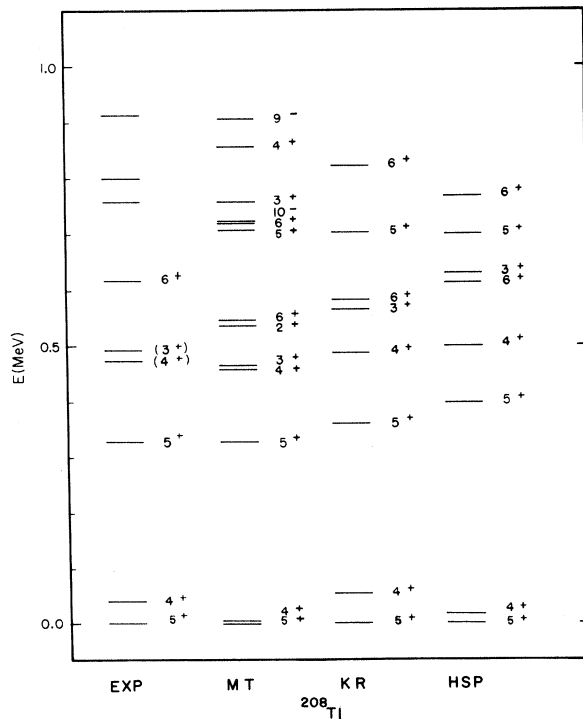


FIG. 11. Comparison of the experimentally observed energy levels (Ref. 63) of ^{208}Tl below 1.0 MeV with the calculations of MT, KR, and HSP.

calculations of HSP,¹⁵ and FG,¹⁹ and HKII²² in Fig. 12.

Recent studies via the $^{208}\text{Pb}(d, \alpha)^{206}\text{Tl}$ reaction by Lewis and Daehnick⁴⁴ and via the $^{205}\text{Tl}(d, p)^{206}\text{Tl}$ reaction by Erskine³¹ have resolved many of the low-lying states in ^{206}Tl and these authors have tentatively assigned spins to their observed levels. Theoretically one would expect to find a low-lying doublet with spins of $J=0^-$ and $J=1^-$ arising principally from the $\bar{s}_{1/2}\bar{p}_{1/2}$ configuration. Experimentally this does not appear to be the case. The ground state which is assigned a spin of $J=0^-$ is well separated from the assigned $J=2^-$ and $J=1^-$ doublet at 263 and 305 keV, respectively. Above this doublet is another $J=2^-$ and $J=1^-$ doublet at 635 and 650 keV, respectively, where the spins and parities have been taken from the work of Lewis and Daehnick.⁴⁴

As can be seen from Fig. 12, none of the theoretical calculations seem to fit this sequence of levels. MT, HSP, and HKII all have the lowest $J=1^-$ level about 200 keV below the first doublet and only about 100 keV above the ground state. FG who use a Tabakin potential find the lowest $J=1^-$ level a little higher at 170 keV but fail to fit the second doublet near 642 keV.

It should be pointed out that the position of the lowest $J=1^-$ level is rather insensitive to the P_2 and P_3 multipole strengths. Providing the experimental results are correct, it is difficult to understand why all shell-model calculations do so poorly

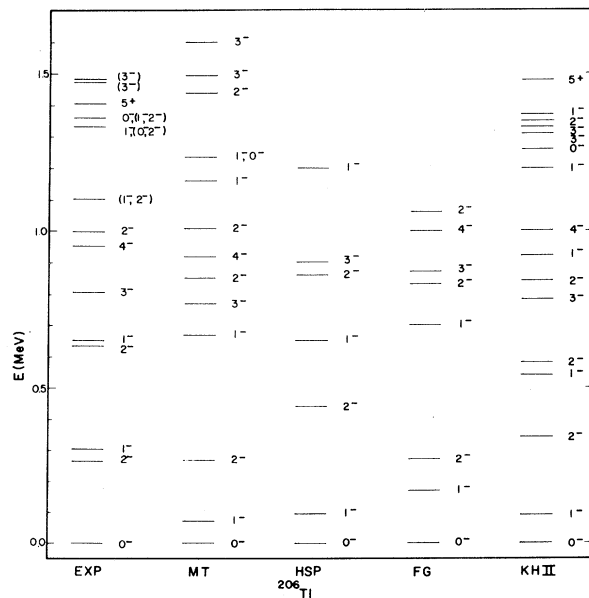


FIG. 12. Comparison of the experimentally observed energy levels (Ref. 44) of ^{206}Tl below 1.5 MeV with the calculations of MT, HSP, FG, and HKII.

in ^{206}Tl while doing so well for the other nuclei in the lead region.

I. ^{206}Hg

The low-lying levels of ^{206}Hg most likely can be described by two proton holes in the ^{208}Pb core. Practically nothing is known about ^{206}Hg except the binding energy of the ground state which is assigned a spin of $J=0^+$. Consequently, no comparison between theory and experiment can be made except for the binding energy as was done in Table II. Since no excited levels are known experimentally, no information could be used to establish the best values for the P_2 and P_3 multipole strengths. Therefore, the P_2 and P_3 strengths were assumed to be the average of the respective strengths of the three like-particle nuclei ^{208}Pb , ^{210}Pb , and ^{210}Po and are given in Table I. Using this residual force, the calculated levels for ^{206}Hg are compared in Fig. 13 with the HKII²² calculated levels.

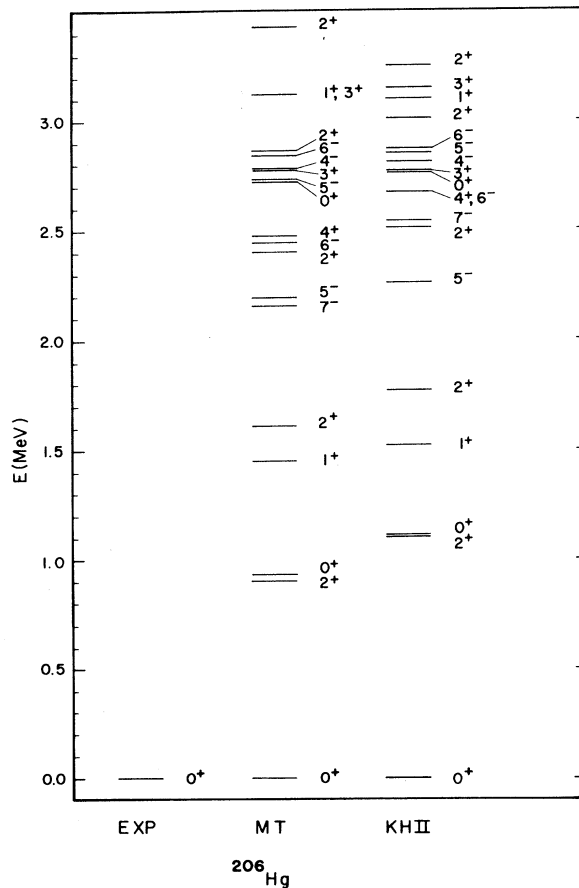


FIG. 13. Comparison of the energy levels of ^{206}Hg below 3.5 MeV of the calculations of MT and HKII.

correctly predicted by KR and HSP using carefully chosen tensor forces. This 0^- level may be one of the few levels in this region which depends sensitively on the explicit use of the tensor force—but the HKII and FG calculations do not support this conclusion. The inability of the present calculations to obtain the correct ordering of the $J=0^-$ and $J=1^-$ levels is probably due to model-space-truncation effects which cannot be assimilated by a simple residual force.

It is seen that most of the low-lying states of nuclei around ^{208}Pb and including ^{208}Pb (TMP) are described by conventional shell-model calculations which use a central Gaussian-shaped interaction plus P_2 and P_3 multipole forces with singlet-even and triplet-even projection operators. On the other hand, the high-lying levels are quite often less satisfactorily described. The present approach tries to account for the effects of model-space truncation by renormalization of the residual force through adjustment of the force parameters which then remain the same for all states within a given nucleus. This approach is workable provided the effects of the model-space truncation are not strongly state-dependent. In the higher-energy regions where “core excitations” are ener-

getically possible, the effects of model-space truncation are more likely to be state-dependent. Hence, within the present model space used, it probably will be very difficult to describe both the low-lying levels and high-lying levels of a given nucleus by merely adjusting the force parameters. There is also evidence indicating that the present model space should be enlarged in order to account for more of the observed data such as the observed $E1$ transitions (which are forbidden in our model space) between the high-lying states in ^{206}Pb and the number of the observed $J=3^-$ and $J=5^-$ levels in ^{206}Pb and ^{210}Po which is greater than can be predicted with the present model space. Since “core excitations” will become increasingly important for the higher-lying levels, a much better treatment of these “core excitations” should be done in order to obtain better description of the higher levels.

Tables have been prepared giving the major amplitudes of the low-lying states of the eight nuclei discussed in this paper. A limited number of these tables are available and may be obtained by writing to William W. True, Physics Department, University of California, Davis, California 95616.

-
- *Work supported in part by a grant from the National Science Foundation and by a grant from the U. S. Atomic Energy Commission.
- †Present address is Physics Department, Indiana University, Bloomington, Indiana 47401.
- ¹W. W. True, C. W. Ma, and W. T. Pinkston, *Phys. Rev. C* **3**, 2421 (1971). This paper will be called TMP in the text.
- ²W. W. True and K. W. Ford, *Phys. Rev.* **109**, 1675 (1958).
- ³W. W. True, *Phys. Rev.* **168**, 1388 (1968).
- ⁴N. Newby and E. J. Konopinski, *Phys. Rev.* **115**, 434 (1959).
- ⁵V. N. Guman, Y. I. Kharitonov, L. A. Sliv, and G. A. Sogomonova, *Nucl. Phys.* **28**, 192 (1961).
- ⁶Y. I. Kharitonov, L. A. Sliv, and G. A. Sogomonova, *Nucl. Phys.* **28**, 210 (1961).
- ⁷R. Arvieu and M. Veneroni, *Phys. Lett.* **5**, 142 (1963).
- ⁸L. S. Kisslinger and R. A. Sorensen, *Rev. Mod. Phys.* **35**, 853 (1963).
- ⁹Y. E. Kim and J. O. Rasmussen, *Nucl. Phys.* **47**, 184 (1963); **61**, 173 (1965).
- ¹⁰Y. E. Kim and J. O. Rasmussen, *Phys. Rev.* **135**, B44 (1964).
- ¹¹M. G. Redlich, *Phys. Rev.* **138**, B544 (1965).
- ¹²B. L. Birbrair and V. N. Guman, *Yad. Phys.* **1**, 971 (1965) [transl.: *Sov. J. Nucl. Phys.* **1**, 693 (1965)].
- ¹³D. Clement and E. Baranger, *Nucl. Phys.* **89**, 145 (1966).
- ¹⁴A. Plastino, R. Arvieu, and S. A. Moszkowski, *Phys. Rev.* **145**, 837 (1966).
- ¹⁵T. A. Hughes, R. Snow, and W. T. Pinkston, *Nucl. Phys.* **82**, 129 (1966).
- ¹⁶T. T. S. Kuo, *Nucl. Phys.* **A122**, 325 (1968).
- ¹⁷C. Riedel, R. A. Broglia, and A. Miranda, *Nucl. Phys.* **A113**, 503 (1968).
- ¹⁸N. Freed and W. Rhodes, *Nucl. Phys.* **A126**, 481 (1969).
- ¹⁹N. Freed and J. G. Gibbons, *Nucl. Phys.* **A136**, 423 (1969).
- ²⁰J. Hadermann and K. Alder, *Helv. Phys. Acta* **42**, 497 (1969).
- ²¹J. Vary and J. N. Ginocchio, *Nucl. Phys.* **A166**, 479 (1971).
- ²²G. H. Herling and T. T. S. Kuo, *Nucl. Phys.* **A181**, 113 (1972); T. T. S. Kuo and G. H. Herling, *NRL Memorandum Report No. 2258*, 1971 (unpublished).
- ²³D. Clement and T. Harvey, *Nucl. Phys.* **A176**, 592 (1971).
- ²⁴D. E. Alburger and M. H. L. Pryce, *Phys. Rev.* **95**, 1482 (1954).
- ²⁵P. Mukherjee and B. L. Cohen, *Phys. Rev.* **127**, 1284 (1962).
- ²⁶J. R. Erskine, W. W. Buechner, and H. A. Enge, *Phys. Rev.* **128**, 720 (1962).
- ²⁷P. Mukherjee, *Phys. Rev.* **131**, 2162 (1963).
- ²⁸W. C. Cobb, *Phys. Rev.* **132**, 1693 (1963).
- ²⁹J. R. Erskine, *Phys. Rev.* **135**, B110 (1964).
- ³⁰P. Weinzierl, E. Ujlaki, G. Preinreich, and G. Eder, *Phys. Rev.* **134**, B257 (1964).
- ³¹J. R. Erskine, *Phys. Rev.* **138**, B851 (1965).
- ³²R. Benoit, G. Bertolini, and F. Cappellani, and G. Res-telli, *Nuovo Cimento* **49B**, 125 (1967).

- ³³G. M. Reynolds, J. R. Maxwell, and N. M. Hintz, *Phys. Rev.* **153**, 1283 (1967).
- ³⁴E. R. Flynn, G. J. Igo, R. Woods, P. D. Barnes, and N. K. Glendenning, *Phys. Rev. Lett.* **19**, 798 (1967).
- ³⁵R. Tickle and J. Bardwick, *Phys. Rev.* **166**, 1167 (1968).
- ³⁶P. Richard, N. Stein, C. D. Kavaloski, and J. S. Lilley, *Phys. Rev.* **171**, 1308 (1968).
- ³⁷S. M. Smith, C. Moazed, A. M. Bernstein, and P. G. Roos, *Phys. Rev.* **169**, 951 (1968).
- ³⁸S. G. Prussin and J. M. Hollander, *Nucl. Phys.* **A110**, 176 (1968).
- ³⁹J. H. Bjerregaard, O. Hansen, O. Nathan, L. Vistisen, R. Chapman, and S. Hinds, *Nucl. Phys.* **A113**, 484 (1968).
- ⁴⁰M. Bonitz, J. Kantele, and N. J. S. Hansen, *Nucl. Phys.* **A115**, 219 (1968).
- ⁴¹G. R. Hagee, R. C. Lange, and A. R. Campbell, *Nucl. Phys.* **A135**, 225 (1969).
- ⁴²T. Yamazaki, *Phys. Rev. C* **1**, 290 (1970).
- ⁴³P. L. Reeder, *Phys. Rev. C* **1**, 721 (1970).
- ⁴⁴M. B. Lewis and W. W. Daehnick, *Phys. Rev. C* **1**, 1577 (1970).
- ⁴⁵S. M. Smith, P. G. Roos, A. M. Bernstein, and C. Moazed, *Nucl. Phys.* **A158**, 497 (1970).
- ⁴⁶G. Igo, E. R. Flynn, B. J. Dropesky, and P. D. Barnes, *Phys. Rev. C* **3**, 349 (1971).
- ⁴⁷W. P. Alford, J. P. Schiffer, and J. J. Schwartz, *Phys. Rev. C* **3**, 860 (1971).
- ⁴⁸H. T. Motz, E. T. Journey, E. B. Shera, and R. K. Sheline, *Phys. Rev. Lett.* **26**, 854 (1971).
- ⁴⁹R. Tickle and J. Bardwick, *Phys. Lett.* **36B**, 32 (1971).
- ⁵⁰C. Ellegaard, P. D. Barnes, E. R. Flynn, and G. J. Igo, *Nucl. Phys.* **A162**, 1 (1971).
- ⁵¹J. Blomqvist, B. Fant, K. Wikstrom, and I. Bergstrom, *Phys. Scr.* **3**, 9 (1971).
- ⁵²G. M. Crawley, W. A. Lanford, D. Kashy, and H. G. Blosser, private communication.
- ⁵³W. A. Lanford, W. P. Alford, and H. W. Fulbright, to be published.
- ⁵⁴L. J. Jardine, S. G. Prussin, and J. M. Hollander, *Nucl. Phys.* **A190**, 261 (1972).
- ⁵⁵P. D. Barnes, E. R. Flynn, G. J. Igo, and D. D. Armstrong, *Phys. Rev. C* **1**, 228 (1970).
- ⁵⁶The $V_0 = -22.75$ MeV in this paper represents the αV_0 strength in Ref. 1.
- ⁵⁷K. H. Maier, K. Nakai, J. R. Leigh, R. M. Diamond, and F. S. Stephens, *Nucl. Phys.* **A183**, 289 (1972).
- ⁵⁸L. J. Jardine, LBL Report No. 246, 1971 (unpublished).
- ⁵⁹G. M. Temmer, in *Proceedings of the International Conference on Nuclear Physics, Gatlinburg, Tennessee, 1966*, edited by R. L. Becker, C. D. Goodman, P. H. Stelson, and A. Zucker (Academic, New York, 1967), p. 223.
- ⁶⁰J. C. Manthuruthil, D. C. Camp, A. V. Ramayya, J. H. Hamilton, J. J. Pinajian, and J. W. Doornebas, *Phys. Rev. C* **6**, 1870 (1972).
- ⁶¹P. D. Barnes, G. Igo, and G. R. Flynn, to be published, as quoted by Ellegaard *et al.* in Ref. 50.
- ⁶²C. Ellegaard, P. D. Barnes, R. Eisenstein, and T. R. Canada, *Phys. Lett.* **35B**, 145 (1971).
- ⁶³C. M. Lederer, J. M. Hollander, and L. Perlman, *Table of Isotopes* (Wiley, New York, 1967), 6th ed.
- ⁶⁴J. G. Beery, Los Alamos Scientific Laboratory Report No. LA-3958, as quoted by C. E. Watson and D. Wright, *Nucl. Phys.* **A188**, 33 (1972).
- ⁶⁵J. J. Kolata and W. W. Daehnick, *Phys. Rev. C* **5**, 568 (1972).
- ⁶⁶C. K. Cline, W. P. Alford, H. E. Gove, and R. Tickle, *Nucl. Phys.* **A186**, 273 (1972).
- ⁶⁷R. D. Lawson, Rutherford Centennial Conference, Christchurch, New Zealand, July 7, 1971.
- ⁶⁸M. H. Macfarlane, *Reaction Matrix in Nuclear Shell Theory, Proceedings of the International School of Physics "Enrico Fermi," Course XL* (Academic, New York, 1969).
- ⁶⁹T. T. S. Kuo, private communication; T. T. S. Kuo and G. E. Brown, in *Proceedings of the International Conference on Nuclear Physics, Gatlinburg, Tennessee, 1966*, (see Ref. 59), p. 526.
- ⁷⁰M. H. Macfarlane and J. B. French, *Rev. Mod. Phys.* **32**, 567 (1960).
- ⁷¹V. Gillet, A. M. Green, and E. A. Sanderson, *Nucl. Phys.* **88**, 321 (1966).